Contribution à "Relativistic Heavy Ion Collisions"
dans le série "International Reviews of Nuclear Physics"
Editeurs D. Strottmann et L.P. Csernai, World Scientific Company,
1991, pp 37-80

Rapport DPh-N/Saclay n°2559 B 05/1989

THE INTRANUCLEAR CASCADE AND THE COLLISION DYNAMICS

D. L'Hôte

Service de Physique Nucléaire à Moyenne Energie, CEN Saclay,
91191 Gif sur Yvette, France

J. Cugnon

Université de Liège, Physique Nucléaire Théorique,
Institut de Physique Sart Tilman, 4000 Liège,
Belgique

THE INTRANUCLEAR CASCADE AND THE COLLISION DYNAMICS

D. L'HÔTE,
CEN - Saclay, DPhN-ME,
F-91191 GIF-SUR-YVETTE Cédex (France)

and

J. CUGNON,
Université de Liège, Physique Nucléaire Théorique, Institut de Physique au
Sart Tilman, Bâtiment B.5,
B-4000 LIEGE 1 (Belgique)

ABSTRACT : The intranuclear cascade model for relativistic heavy ion collisions is reviewed. A comparison between the codes developed by various groups is made. The theoretical foundation of the intranuclear cascade is discussed. The features of the collision dynamics, embodied by the intranuclear cascade, are briefly described, as well as the limiting regimes. A comparison of the most important predictions of the model with experiment is presented. The role of the viscosity in flow properties is emphasized. The connection with mean field theories is shortly discussed, as well as the potentialities of the simulation method for describing correlations and fluctuations.

1. INTRODUCTION

The intranuclear cascade (INC) has been invented by Serber[1] forty years ago to handle the multiple scattering of an incident particle (a proton in this case) inside a nucleus. As for the extra-nuclear cascade, i.e. the multiple

scattering of an incident particle from nucleus to nucleus inside a thick target, he used a simulation procedure. Thus the most general definition of the INC is the simulation of multiple scattering inside nuclei. Although the method turned out to be very successful from the beginning, it raised several problems : (i) it is based on numerical simulation and therefore relies on large statistics ; (ii) it obviously neglects quantum interference effects, even if the latter are probably decreasing as the number of collisions increases ; (iii) its connection with basic theory is not well clarified. In other words, it is not known which equation is exactly solved by the INC and to what degree of approximation.

Initially used to describe hadron-nucleus interactions in the GeV range, the INC model was extended to heavy ion collisions in the GeV/u range, where it reveals itself as a powerful tool of investigation. We will concentrate here to this kind of problem, but we have to mention that the INC has since been used in many different systems as well as in different energy ranges.

The physics handled by the INC model is the non-equilibrium dynamics of many-fermion systems dominated by two-body collisions. This dynamics was known for a long time in some special limit : relaxation time limit, short mean free path limit,... in extended systems essentially. The INC allows to handle any non-equilibrium situation, including the possible creation or destruction of mesons. In recent extensions of the INC to lower energies, one was forced to introduce a time-dependent mean field. This led to a variety of new models (VUU, BUU, "Landau-Vlassov",...), but the collision dynamics was basically kept the same as in the INC. The physical motivation was the handling of compression effects, hopefully linked with the nuclear equation of state.

In this review, we basically describe the INC approach which follows the paths of all particles in phase space at the same time and insist on its relevance to the collision dynamics. In section 2, we explain in some detail the INC model and discuss its range of validity as well as its basic physical input. In section 3, we investigate the connection with theory. Section 4 is devoted to an extensive discussion of the various features of the collision dynamics, including the relationship with known limits and similarity theory. In section 5, we review the most important physical results which have been obtained or enlightened with the help of the INC. Section 6 discusses new perspectives and section 7 contains the conclusion.

2. THE INC MODEL

2.1. Preliminaries

In simple words, the INC model is a method to handle quantum multiple scattering involving many-fermion systems, including creation and absorption of mesons. In other words, the INC model pictures the interaction processes by a simulation of a time-ordered sequence of (usually) binary collisions. A good description of the basic concepts, as well as a review of the various methods may be found in ref. [2]. Depending upon one is especially interested in the time evolution of the whole system or in the dynamical story of a cascading particle, the model has been based on the minimum relative distance for two colliding particles (this is the case for most of the well celebrated codes used in heavy ions) or on the concept of mean free path (this has been used mainly in hadron-nucleus collisions).

2.2. Simulation based on minimum distance of approach

This method has been given a simple though powerful form in ref. [3], but was used previously in refs. [4-10] and later on by several groups[11-13]. The idea is the following : (a) the nuclei are prepared by picking up at random position and momentum of the nucleons according to density and Fermi distributions. The target is boosted by a Lorentz transformation ; (b) nucleons travel along straight line trajectories until two of them reach their minimum distance of approach d_{min} . At this time, d_{min} is checked with the total cross-section σ at the c.m. energy $\sqrt{s}$ of the colliding pair. If $d < \sigma(\sqrt{s})$, the two particles are forced to scatter. The final state (if many of them are possible) is chosen at random in proportion of the partial cross-sections. The final momentum of the particles are constructed in accordance with momentum-energy conservation laws and with experimental differential cross-section. This is easily realized in the c.m. frame where the c.m. momentum is easily calculated and where simply the polar angle Θ is to be determined randomly with a probability law following the experimental differential cross-section. Of course, if $d > \sigma(\sqrt{s})$, nothing is changed. The straight line motion is then resumed until another pair reaches its minimum distance of approach ; (c) the process is stopped when the binary collisions cease (in practice, when the collision rate is low enough) or when a physical criterion is met. The procedure is repeated by changing the realization of the initial state. One so generates N_{ev} "events". Physical quantities (including observables) are calculated by ensemble averages.

Many other features should be given in order to complete the description of the model. They have been included progressively with time. We list the most important here.

1. Inelastic processes are introduced by the isobar picture : the processes

$$N + N \rightleftarrows N + \Delta \qquad (2.1)$$

$$\Delta \rightleftarrows \pi N \qquad (2.2)$$

were introduced from the beginning. The cross-section for the direct process (2.1) was estimated as accounting for the experimental inelastic cross-section. The cross-section for the reverse process $\Delta N \rightarrow NN$ is calculated by detailed balance (see ref. [8] for detail). The $\pi N \rightarrow \Delta$ cross-section is taken as the experimental total (basically elastic) πN cross-section. The Δ-decay is dictated by the experimental lifetime of the resonance. In the $NN \rightarrow N\Delta$ process, the mass of the delta was determined randomly with a Lorentzian distribution (with parameters borrowed from experiment $M_0 \approx 1.230$ GeV, $\Gamma \approx 0.120$ GeV) in agreement with available energy (see ref. [11] for detail).

2. Pauli principle is taken into account by checking phase space occupation around the collision location. If the latter is $\bar{f}$ (for each of the nucleons) the collision is realized if a random number is less than $1 - \bar{f}$.

3. Isospin is taken into account (see ref. [11]).

4. Binding. In the absence of mean field effect, the cohesion of the nuclei is ensured by freezing the Fermi motion. The latter is restored for any of the nucleons once it is going to make its first collision. Some amount of energy is removed before the final energy of a particle is compared with experiment. In the simplest cases, a fixed amount of energy is removed at the end. But in the code of ref. [13], it can be removed at any time, if the particles leave the (freely) moving potential wells assumed to travel with the nuclei.

5. Relativistic kinematics is used. Relativistic invariance is however not guaranteed, although an invariant minimum distance of approach is introduced.

6. Additional processes have sometimes been included, like :

$$\pi N \rightarrow \pi\pi N \,,\ \Delta\Delta \rightarrow \Delta\Delta \,,\ \Delta N \rightarrow \Delta N \,,\ \pi NN \rightarrow NN \,,\ \pi N \rightarrow \pi N \,,\ldots \,. \qquad (2.3)$$

especially in the context of $\bar{p}$-nucleus interaction[14].

2.3. Simulation based on mean free path

The basic idea, originally used by Serber[1] and adopted by many authors[15-23], is to determine the free path ℓ of an incoming particle as randomly given by an exponential law

$$P(\ell) = \exp(-\rho\,\ell\,\sigma) \qquad (2.4)$$

where ρ is the medium density and σ the cross-section. If the density ρ is varying the optical length is used. At the end of the free path, the incident particle is assumed to make a collision with one of the nucleons. The latter is promoted, it is to say its motion is then followed in detail and it is also given a mean free path. A hole is then punched in the medium. The tree-like structure of the cascade is so constructed. Remark that a cascading particle always sees a continuous medium except if it is pushed backwards.

For the heavy ion (and for the antiproton) case, the incident particles were originally considered as cascading independently. Later on, the so-called interaction between cascades was introduced. In ref. [18], this was realized as "if a cascade produced a depopulated medium for the particles of another cascade". In ref. [23], the cascades are progressing altogether as in the codes of category 2.2, but everything is still based upon mean free path.

2.4. Mathematical output

Forgetting for a while the production processes, the output of an "event" is a collection of 6A functions of time

$$\{\vec{r}_1,\ldots,\vec{r}_A\,,\,\vec{p}_1,\ldots,\vec{p}_A\}\,,\ \vec{r}_1 = \vec{r}_1(t,\zeta)\,,\ \vec{r}_2 = \vec{r}_2(t,\zeta)\,,\ldots,\ \vec{p}_A = \vec{p}_A(t,\zeta)\,. \qquad (2.5)$$

where ζ is the label of the runs and can be viewed as representing stochasticity, (both in the description of the initial state and of the binary collisions). From these functions (mainly step functions), one may build the one-body distribution function

$$f_1(\vec{r}\,,\vec{p}\,,t) = N_{ev}^{-1}\sum_{\zeta}\sum_{i=1}^{A}\delta(\vec{r}-\vec{r}_i)\,\delta(\vec{p}-\vec{p}_i) \qquad (2.6)$$

the two-body distribution function as

$$f_2(\vec{r}\,,\vec{p}\,,\vec{r}\,',\vec{p}\,',t) = N_{ev}^{-1}\sum_{\zeta}\sum_{i=1}^{A}\sum_{j\neq i}\delta(\vec{r}-\vec{r}_i)\,\delta(\vec{r}\,'-\vec{r}_j)\,\delta(\vec{p}-\vec{p}_i)\,\delta(\vec{p}\,'-\vec{p}_j) \qquad (2.7)$$

and all the distribution functions up to the A-body distribution function

$$f_A(\vec{r}, \vec{p}, ..., \vec{r}^A, \vec{p}^{(A)}, t) = N_{ev}^{-1} \sum_{\zeta} \sum_{i_1=1}^{A} \sum_{i_2 \neq i_1} \sum ... \delta(\vec{r} - \vec{r}_{i_1}) ... \delta(\vec{r}^{(A)} - \vec{r}_{i_A})$$

$$\delta(\vec{p} - \vec{p}_{i_1}) ... \delta(\vec{p}^{(A)} - \vec{p}_{i_A}) . \qquad (2.8)$$

Obviously, the distribution functions are normalized as :

$$\int d^3r\, d^3p\, f_1(\vec{r}, \vec{p}, t) = A , \qquad (2.9a)$$

$$\int d^3r\, d^3p\, d^3r'\, d^3p'\, f_2(\vec{r}, \vec{p}_2, \vec{r}', \vec{p}_1, t) = A(A-1) , \qquad (2.9b)$$

and so on. For obvious reasons, only the lowest order functions can be evaluated reliably. In practice the delta function in eqs. (2.6)-(2.8) are replaced by step functions defined on a mesh in phase space.

2.5. Relation with experiment

The relation between calculated distribution functions and the observables is a delicate question, common to all transport theories, for two main reasons : (i) first, they do not intrinsically incorporate a dynamics for the formation of clusters (this has to be supplemented by some external, ad hoc, procedure) ; (ii) experimental data are obtained with the help of detectors, plagued by some acceptance, which depends upon the nature of the clusters. Symbolically, and in all generality, an observable involving a s-body operator (in phase space) can be represented by

$$O_s = \frac{1}{N_{ev}} \sum_{\zeta} \hat{O}_s(1,...,s)\, L_A L_C \{\vec{r}_1(t,\zeta),...,\vec{p}_A(t,\zeta)\} , \qquad (2.10)$$

where L_C realizes the clusterization in event labelled ζ, L_A represents the cuts typical of the detector, $\hat{O}_s$ is the appropriate s-body operator taken at $t \to \infty$ and the summation runs over the number of events. In general L_A and L_C are not linear operators. Therefore the observables cannot be expressed in terms of the distribution functions. Furthermore, the detectors are such that the operator L_A can depend crucially on slight differences in the results of L_C, at least for some observables (e.g. if the detectors have different thresholds in velocity for α particles and deuterons, a small modification in L_C can give different results for an α-particle and for two deuterons travelling with the same velocity). This is the case for the so-called (see ref. [24]) flow angle.

Sometimes, it is possible to get rid of the uncertainties of L_A (large perpendicular momentum at forward angles). Still, the operation O_s does not commute with L_C and may still depend on its action. In some cases, it is possible to consider observables which are almost clusterization-independent. The most common of them is the so-called quasi-proton invariant cross-section, which can be written as (ζ running over all impact parameters b, σ_r being the total reaction cross-section) :

$$E\frac{d^3\tilde{\sigma}}{dp^3} = \frac{\sigma_r}{N_{ev}} \sum_{\zeta} \lim_{t \to \infty} \sum_{i=1}^{A} \frac{1}{2}(1 + \tau_{3i})\, E\, \delta(\vec{p} - \vec{p}_i(t,\zeta)) , \qquad (2.11)$$

which is equivalent to :

$$E\frac{d^3\tilde{\sigma}}{dp^3} = 2\pi \int_0^{\infty} bdb \lim_{t \to \infty} \int d^3r E\, \hat{f}_{1(b)}(\vec{r}, \vec{p}, t) , \qquad (2.12)$$

where the b-dependence of the one-body distribution for participant protons has been explicitly introduced. This can be identified to the experimental quantity :

$$E\frac{d^3\tilde{\sigma}}{dp^3} = E\frac{d^3\sigma_p}{dp^3} + 4\, E_d \left(\frac{d^3\sigma_d}{d^3p_d}\right)_{p_d = 2p} + 9\, E_t \left(\frac{d^3\sigma_t}{d^3p_t}\right)_{p_t = 3p} + ... \qquad (2.13)$$

where all the species are summed up. Equivalence of eqs. (2.11) and (2.12) follows from the asymptotic ($t \to \infty$) form of f_1 :

$$f_1(\vec{r}, \vec{p}, t) \sim \phi(\vec{p})\, \psi(\vec{r} - \frac{\vec{p}}{m} t) . \qquad (2.14)$$

The factorization occurs after all collisions are over. Similar expressions can be obtained for two-particle correlations and for deuteron production. For the latter, the authors of ref. [25] give (ζ including all b's) :

$$E_d \frac{d^3\tilde{\sigma}}{dp_d^3} = \frac{3}{4} \frac{\sigma_r}{N_{ev}} \sum_\zeta \sum_{i<j} \frac{1}{4} (1 + \tau_{3i})(1 - \tau_{3j}) E_d \int d^3r \int d^3p \, g_d(\vec{r}, \vec{p})$$

$$\delta(\vec{p}_d - \vec{p}_i(t,\zeta) - \vec{p}_j(t,\zeta)) \, \delta(\vec{r} - \vec{r}_i(t,\zeta) + \vec{r}_j(t,\zeta)) \, \delta\left(\vec{p} - \frac{\vec{p}_i}{2}(t,\zeta) + \frac{\vec{p}_j}{2}(t,\zeta)\right) \quad , \quad (2.15)$$

where t is the time at the freeze-out and where g_d is the deuteron wave function in Wigner representation. Formula (2.15) amounts to count all p-n pairs with the required total momentum and with a relative position in phase space which resembles, at the freeze-out time, the internal structure of a deuteron. Of course, this involves an implicit model for deuteron formation. If there is no two particle correlation ($f_2 = f_1 f_1$), expression (2.15) is equivalent to :

$$E_d \frac{d^3\tilde{\sigma}}{dp_d^3} = 2\pi \int b \, db \, \frac{3}{4} E_d \int d^3r \int d^3p \, g_d(\vec{r}, \vec{p}) \, f_1^{(p)}(\vec{r}_1, \vec{p}_1, t) \, f_1^{n}(\vec{r}_2, \vec{p}_2, t)$$

$$\delta(\vec{p}_d - \vec{p}_1 - \vec{p}_2) \, \delta\left(\vec{p} - \frac{\vec{p}_1}{2} + \frac{\vec{p}_2}{2}\right) . \quad (2.16)$$

Both in eqs. (2.15) and (2.16), the factor 3/4 accounts for the selection of the proper spin state. According to ref. [25], the cross-section (2.16) should be identified with the experimental quantity

$$E_d \frac{d^3\tilde{\sigma}}{dp_d^3} = E_d \frac{d^3\sigma}{dp_d^3} + \frac{3}{2} \times \left(\frac{3}{2}\right)^2 \left[\left(E_t \frac{d^3\sigma}{dp_t^3} \right)_{p_t = \frac{3}{2} p_d} + \left(E_{^3He} \frac{d^3\sigma}{dp^3_{^3He}} \right)_{p_{^3He} = \frac{3}{2} p_d} \right.$$

$$\left. + 3 \times 4 \left(E_\alpha \frac{d^3\sigma}{dp_\alpha^3} \right)_{p_\alpha = 2p_d} + \ldots \right] , \quad (2.17)$$

i.e. the "effective" deuteron cross-section, be they free or hidden in heavier composites.

2.6. Conditions of validity

Disregarding the problem of the clusterization (or freeze-out), one may inquire about the conditions of validity of the INC picture. This question is very hard and a complete answer can only be given after a proper "derivation" of the INC from basic theory is achieved. Furthermore the dynamics is already rather complex so that a general answer is meaningless. We will concentrate

here on the INC as a classical tool simulating collisions in a gas (the so-called collision regime or Boltzmann limit) and make general considerations.

Quantum motion (wave packets) is neglected. This is certainly not a problem as far as nucleus motion is concerned. For NN motion, the maximum number of partial waves is given by $r_s/\hbar k$ where r_s is range of the force and $\hbar k$ is the typical relative momentum. Around 1 GeV/u, this gives $\ell \leq 3$, which is not very large. This calls for a quantum treatment of the scattering process. Certainly a strict classical description is forbidden, like the equation of motion approach[26-27]. The INC recipe which amounts to keeping a simple trajectory but introducing quantum uncertainty by limited randomness in the scattering process seems to comply with quantum mechanics miraculously.

Quantum interference of collisions is neglected. This restricts in principle to the independent collision regime, which roughly demands :

$$r_s^3 \rho \leq 1 \quad (2.18)$$

where ρ is the actual density. Even for normal nuclear matter, this condition is barely met. Note, however, that many inclusive quantities involve summation over many collisions. Quantum interference effects will then be washed out since they presumably add incoherently. This is not the case for two-proton correlations at small angles for instance[28].

Quantum mechanics affects successive collisions because in a short time interval, particles are put off-shell. Let δt be the time separating two successive collisions. The Heisenberg principle introduces an uncertainty in energy $\delta\varepsilon \approx \hbar/\delta t$, which can be compared to the kinetic energy of the nucleon :

$$\frac{\delta_\varepsilon}{\varepsilon} = \frac{\hbar}{\delta t} \frac{2m_N}{\hbar^2 k^2} \approx \frac{2}{\lambda k} , \quad (2.19)$$

where the mean free path ($\lambda \approx v\delta t$) for collisions is introduced. At 1 GeV/u, typical values of k may be $k \approx 0.5$ GeV/c, which gives $\delta\varepsilon/\varepsilon \approx 40$ %. Note that this effect increases with density ! This quantum effect is always neglected. It can be introduced as retardation effects in the collisions (see section 3), but has retained few attention, except in some academic problems. The apparent unimportance of this effect in the GeV/u range could come from the relative constancy of the cross-section in a broad range.

Note that the INC is not subject to some limitations often encountered by many kinetic methods. It is not Markovian and does not assume homogeneity (in space or time). Furthermore it does not require the famous

"stosszahlansatz" hypothesis, since two-body correlations effects on the phase-space occupancy are taken into account at any time (see section 3.3).

The success of the INC model is quite surprising in view of the above discussion and is still a mystery. It seems that quantum effects are just not showing up and that the main features of the collision process are dictated by the gross features of the microscopic input.

3. RELATION WITH MANY-BODY THEORY

3.1. Introduction

The central problem in nuclear physics in our days is to know what are the "right" degrees of freedom. Are they nucleon, nucleon plus meson or quark plus gluon degrees of freedom ? Furthermore should they be treated classically, quantum mechanically ? The answer depends upon the problem (and the scale) one is looking at. Here we focus on a description in terms of nucleons interacting through potentials (plus pion creation, treated classically), which is the one which has been pushed the most forward, by far. The challenging description would involve a field theory for nucleons plus mesons. But the latter is not very well developed for non-equilibrium situations. Furthermore, it is not sure at all that nucleons can be treated as an ordinary fermion field.

3.2. From many-body theory to transport equation

We thus assume that a system of A nucleons interacting through potentials can be described by a Schrödinger theory. This problem cannot be solved exactly, even with present-day computers. One has then to rely on approximations. The latter are best introduced through the density matrices (BBGKY) hierarchy[29]. Let us denote by $\rho_1, \rho_2, \rho_3, \ldots$ the one-body, two-body, three-body,... density matrices, and let

$$H = \sum_{i=1}^{A} T_i + \sum_{i<j} V_{ij} \qquad (3.1)$$

be the A-body hamiltonian. The Schrodinger equation is equivalent to the following set of equations :

$$i\hbar \frac{\partial \rho_1}{\partial t} = \left[T_1 , \rho_1\right] + \mathop{Tr}_{(2)}\left[V_{12} , \rho_2(1,2)\right] \qquad (3.2)$$

$$i\hbar \frac{\partial \rho_2}{\partial t} = \left[T_1 + T_2 + V_{12} , \rho_2(1,2)\right] + \mathop{Tr}_{(3)}\left[V_{13} + V_{23} , \rho_3(1,2,3)\right] \qquad (3.3)$$

$$\ldots$$

$$i\hbar \frac{\partial \rho_n}{\partial t} = \sum_{i=1}^{n}\left[T_i , \rho_n(1,\ldots,n)\right] + \sum_{i<j}^{n}\left[V_{ij} , \rho_n(1,\ldots,n)\right] + \mathop{Tr}_{(n+1)}\sum_{i=1}^{n}\left[V_{in+1} , \rho_{n+1}(1,\ldots,n+1)\right] , \qquad (3.4)$$

where we have explicitly indicated the particle degrees of freedom in the density matrices and where the symbol $\mathop{Tr}_{(i)}$ means that the trace should be taken on the degrees of freedom of the i^{th} particle. The hierarchy is usually truncated somewhere. The simplest truncation is obtained by assuming

$$\rho_2(1,2) = \rho_1(1)\,\rho_1(2)\,\mathcal{A}_{12} , \qquad (3.5)$$

where $\mathcal{A}_{12}$ is the antisymmetrization operator. The hierarchy then closes on eq. (3.2), which becomes

$$i\hbar \frac{\partial \rho_1}{\partial t} = \left[T_1 + \mathop{Tr}_{(2)} \mathcal{A}_{12} V_{12} \rho_1(2) , \rho_1(1)\right] . \qquad (3.6)$$

The next possible truncation amounts to neglect ρ_3 in eq. (3.3) and assumes that at some time t_0 , ρ_2 is a product of ρ_1's. At later times, ρ_2 will contain the correlations due to one interaction only. The formal solution reads

$$\rho_2(1,2,t) = e^{\frac{i}{\hbar}(T_1 + T_2 + V_{12})(t - t_0)} \rho_2(1,2,t_0)\, e^{-\frac{i}{\hbar}(T_1 + T_2 + V_{12})(t - t_0)} \qquad (3.7a)$$

We next introduce the approximation of taking $\rho_2(1,2,t_0)$ to be uncorrelated and using ρ_2 in first order in V_{12}. This gives :

$$\rho_2(1,2,t) = \rho_1(1)\,\rho_1(2)\,\mathcal{A}_{12} + \frac{1}{E_{12} - T_1 - T_2 + i\varepsilon} V_{12}\,\rho_1(1)\,\rho_1(2)\,\mathcal{A}_{12} - \rho_1(1)\,\rho_1(2)\,\mathcal{A}_{12} V_{12} \frac{1}{E_{12} - T_1 - T_2 - i\varepsilon} \qquad (3.7b)$$

Here the limit $t_0 \to -\infty$ has been taken for introducing conventional scattering

theory. Similarly, outgoing wave boundary conditions have been introduced (hence the ε's in eq. (3.7b)). Approximation (3.7b) applies to the weak coupling limit : very small potentials and collision time much smaller than the mean free time between collisions. The quantity E_{12} should be considered as the energy of the (uncorrelated) state on which the operator $(T_1 + T_2)$ acts. Replacing expression (3.7b) into eq. (3.2), one obtains[30-32]

$$i\hbar \frac{\partial \rho_1}{\partial t} - \left[T_1 + U(1), \rho_1\right] - \mathrm{Tr}_{(2)}\left[V_{12}\mathcal{A}_{12}\rho_1(2)\rho_1(1) - \rho_1(1)\rho_1(2)\mathcal{A}_{12}V_{12}\right]$$
$$+ \mathrm{Tr}_{(2)} V_{12}\mathcal{A}_{12}\rho_1(1)\rho_1(2)V_{12}\frac{1}{E_{12} - T_1 - T_2 - i\varepsilon}$$
$$- \mathrm{Tr}_{(2)}\frac{1}{E_{12} - T_1 - T_2 + i\varepsilon} V_{12}\mathcal{A}_{12}\rho_1(1)\rho_1(2)V_{12} = 0 \ , \qquad (3.8)$$

where

$$U(1) = \mathrm{Tr}_{(2)} V_{12}\mathcal{A}_{12}\rho_1(2) \qquad (3.9)$$

is the mean field. The Green functions in eq. (3.8) can be written as :

$$(E_{12} - T_1 - T_2 \mp i\varepsilon)^{-1} = \mathcal{P}(E_{12} - T_1 - T_2)^{-1} \pm i\pi\,\delta(E_{12} - T_1 - T_2) \ , \qquad (3.10)$$

where $\mathcal{P}$ represents the principal part. Retaining only the imaginary part, one obtains, when writing the operators and the density matrices in Wigner representation :

$$\left\{\frac{\partial}{\partial t} + \frac{1}{m}\left(\vec{p}.\vec{\nabla} - (\vec{\nabla}U).\vec{\nabla}_p + (\vec{\nabla}_p U).\vec{\nabla}\right)\right\} f_1(\vec{r}, \vec{p}, t) =$$

$$\int \frac{d^3p_2}{(2\pi)^3}\frac{d^3p_3}{(2\pi)^3}\frac{d^3p_4}{(2\pi)^3} W(\vec{p}_3\vec{p}_4 \to \vec{p}\,\vec{p}_2)\,\delta(\vec{p} + \vec{p}_2 - \vec{p}_3 - \vec{p}_4)\,\delta\left(e(p) + e(p_2) - e(p_3) - e(p_4)\right)$$

$$\left[\tilde{f}_3\tilde{f}_4(1 - \tilde{f})(1 - \tilde{f}_2) - \tilde{f}\tilde{f}_2(1 - \tilde{f}_3)(1 - \tilde{f}_4)\right] \ , \qquad (3.11)$$

with

$$U(\vec{r}, \vec{p}, t) = \int d^3r'\, d^3p'\, V_{12}(\vec{r} - \vec{r})\, f_1(\vec{r}', \vec{p}', t)$$
$$- \int d^3p' \int \frac{d^3s}{(2\pi)^3} V(\vec{s})\, e^{i(\vec{p} - \vec{p}').\vec{s}}\, f_1(\vec{r}, \vec{p}', t) \ , \qquad (3.12)$$

being the Hartree-Fock mean field in Wigner representation, and

$$W(\vec{p}_3\vec{p}_4 \to \vec{p}\,\vec{p}_2) = \pi\left|<\vec{p}_3\vec{p}_4|V_{12}|\widetilde{\vec{p}\,\vec{p}_2}>\right|^2 \qquad (3.13)$$

and

$$\tilde{f}_i = f_1(\vec{r}, \vec{p}_i, t) \ . \qquad (3.14)$$

The quantity $e(p)$ is equal to $p^2/2m$ in the present limit. Another simplification has been introduced between (3.10) and (3.11), namely high-order derivatives in the mean field have been neglected. Equation (3.11) is the standard form of what is usually considered as a "good" transport equation for nuclear systems. However, it has been advocated that the nuclear case lies beyond the dilute limit. The usual argument is that, in the strong interaction case, two colliding particles interact repeatedly with each other, while their energy may also be modified by the background of the remaining particles, very much in the spirit of Brueckner theory. Botermans and Malfliet[33] have indeed shown that this amounts to keep eq. (3.11) (in the limit of time-locality, see below), while replacing, in the mean field (3.12) and in the transition matrix (3.13), the bare interaction V_{12} by the so-called Brueckner G-matrix

$$G = V_{12} + V_{12}\frac{Q_{ij}}{E_{12} - e(i) - e(j)} G \qquad (3.15)$$

and to include self-energy in the single-particles energies :

$$e(p) = \frac{p^2}{2m} + U(\vec{r}, \vec{p}) \ . \qquad (3.16)$$

They change from point to point. In the derivation of ref. [33], the Pauli operator Q_{ij} acting on the intermediate states i, j should be calculated with the instantaneous momentum distribution. However, it is often proposed to use the local density approximations[33,34] :

$$U_{HF}(\vec{r}, \vec{p}) = U_B(\vec{p}, \rho, T)_{\rho = \rho(\vec{r}),\, T = T(\vec{r})} \ , \qquad (3.17a)$$

$$W<\vec{p}_3\vec{p}_4 \rightarrow \vec{p}\,\vec{p}_2> = \pi \left| <\vec{p}_3\vec{p}_4|G_{12}(\rho\,,T)|\widetilde{\vec{p}\,\vec{p}_2}>\right|^2 , \qquad (3.17b)$$

$$e(p) = \frac{p^2}{2m} + U_B(\vec{p}\,,\rho\,,T) , \qquad (3.17c)$$

where U_B is the single-particle field calculated in uniform matter at density ρ and temperature T within Brueckner theory

$$U_B(\vec{p}) = \sum_{\vec{p}'} n(\vec{p}') <\vec{p}\,\vec{p}'|G|\widetilde{\vec{p}\,\vec{p}'}> . \qquad (3.18)$$

The matrix G reduces to the usual scattering $\mathcal{T}$-matrix if $Q_{ij} \rightarrow 1$. The difference carries medium corrections on the scattering properties.

Equations (3.11) and (3.15)-(3.18) constitute the state of the art in matter of nuclear transport. We recall that they are obtained within the following hypotheses (except for production processes) :

(1) potential interactions
(2) two-body scattering
(3) no higher-order correlation
(4) uncorrelated colliding pairs
(5) no retardation effect (in quantum collisions).

Approximation (3) probably breaks down at high density (and thus at high energy). At low energy, the most serious approximation comes from point (5). The problem has been studied in generality by Baym and Kadanoff[35], and in some particular cases, by Danielewicz[36,37]. The effect can be taken care of by introducing a new (relative) time. The collision term becomes non-local in this time. An alternative more transparent approach introduces a more general distribution function $f(\vec{r}\,,\vec{p}\,,\omega\,,t)$ depending also upon the frequency and the concept of quasi-particle, an object whose energy is not completely determined at any time, but centered around $e(\vec{p})$, introduced in eq. (3.16). The physical origin of this concept is the fact that between collisions, the particle is never "asymptotic". In a model numerical study[37], it is shown that the equilibration rate is reduced by this quantum effect, by ~ 25 % to give a number. It is not clear what is the physical parameter controlling this effect, since the latter basically depends upon the ω-dependence of the function $f(\vec{r}\,,\vec{p}\,,\omega\,,t)$. In equilibrium situation, the ω-dependence is largely dominated by the one of the strength function[38], but this has not been studied very much.

In conclusion, a satisfactory nuclear transport theory, except for the uncertainties mentioned above, seems to be embodied by eq. (3.11) with the medium corrected ingredients, hereafter referred to as the Landau-Vlassov equation. The INC model can handle this equation with exception of the mean field (related to compression) effects : that is what we call here the collision dynamics, which largely dominates in heavy ion physics. The treatment of mean field requires going from linear trajectories to curvilinear trajectories between collisions. This is done in the VUU and so-called Landau-Vlassov methods, in full development these days[39-46].

3.3. Does simulation solve the transport equation ?

This question has been addressed by several authors. The real question is : do we solve eq. (3.11) (for U = 0) by the simulation procedure described in section 2.2 ? The answer is no for an obvious reason : the probability for having a collision in the cascade depends upon the joint probability of finding two particles close in phase space, a quantity directly related to the two particle distribution function f_2 . Therefore one expects rather an equation of the type :

$$\mathcal{L}_1^{(0)} f_1(\vec{r}\,,\vec{p}\,,t) = \int \frac{d^3p_2}{(2\pi)^3}\frac{d^3p_3}{(2\pi)^3}\frac{d^3p_4}{(2\pi)^3}\Big[W(\vec{p}_3\vec{p}_4 \rightarrow \vec{p}\,\vec{p}_2) f_2(\vec{r}\,,\vec{p}_3\,,\bar{r}\,,\vec{p}_2\,,t)(1-\bar{f}_2)(1-\bar{f}$$

$$- W(\vec{p}\,\vec{p}_2 \rightarrow \vec{p}_3\vec{p}_4) f_2(\vec{r}\,,\vec{p}\,,\bar{r}\,,\vec{p}_2\,,t)(1-\bar{f}_3)(1-\bar{f}_4)\Big] , \qquad (3.19)$$

where $\mathcal{L}_s^{(0)}$ is the independent s-body Liouvillian

$$\mathcal{L}_s^{(0)} = \frac{\partial}{\partial t} + \sum_{j=1}^{s} \frac{\vec{p}_j}{m}\cdot\vec{\nabla}_j , \qquad (3.20)$$

and where a $\bar{r}$ has been introduced in the collision integral to indicate symbolically that the INC does not demand a strict locality. We conjecture here that the INC model is equivalent to solving the hierarchy formed by eq. (3.19), the following equation

$$\mathcal{L}_2^{(0)} f_2(\vec{r}_1, \vec{p}_1, \vec{r}_2, \vec{p}_2, t) =$$

$$\int \frac{d^3p'}{(2\pi)^3}\frac{d^3p_3}{(2\pi)^3}\frac{d^3p_4}{(2\pi)^3}\Big[W(\vec{p}_3\vec{p}_4 \to \vec{p}_1\vec{p}')f_2(\vec{r}, \vec{p}_3, \vec{r}, \vec{p}_4, t)(1-\hat{f}_1)(1-\hat{f}')$$

$$+ W(\vec{p}_3\vec{p}_4 \to \vec{p}'\vec{p}_2)f_2(\vec{r}, \vec{p}_3, \vec{r}, \vec{p}_4, t)(1-\hat{f}')(1-\hat{f}_2)$$

$$- W(\vec{p}_1\vec{p}' \to \vec{p}_3\vec{p}_4)f_2(\vec{r}, \vec{p}, \vec{r}, \vec{p}', t)(1-\hat{f}_3)(1-\hat{f}_4)$$

$$- W(\vec{p}', \vec{p}_2 \to \vec{p}_3\vec{p}_4)f_2(\vec{r}, \vec{p}, \vec{r}, \vec{p}', t)(1-\hat{f}_3)(1-\hat{f}_4)\Big] , \qquad (3.21)$$

and similar higher-order equations that we do not write down, but that are characterized by the fact that the s-body distribution functions entering the collision term are factorized into s-2 and 2-body distribution functions. In other words, the INC amounts to collect for the evolution of any s-body distribution function the effect of the two-body correlation function on the collision term. The relation of the INC algorithm and eq. (3.19) has been studied by Bunakov (see ref. [47]) and references cited therein), who considered slightly different transport equations, but having the same structure (see also ref. [48]). We will not enter into the detail here. But we mention that it has been shown that the INC simulation amounts to evaluate the collision integral by a Monte-Carlo method. But this result is only obtained in the limit of a large number of collisions. This may be understood as follows : in a given run the sequence of collisions depends upon realization (by random choices) of the whole system, i.e. of the A-body distribution function. Therefore, a large number of runs give a good sample of the one- (and two-) body distribution function, but the probabilities are not totally independent of distribution functions. Lately, this problem was attacked[49] for the case of a soluble, through rather academic model. It was shown that the INC algorithm solves the collision integral in the dilute case (eq. (2.18)) only. The situation may be cured by the so-called quasi-particle method : replacing a nucleon by N particles (with weight 1/N) interacting through σ/N instead of σ. It is easily checked that the scaling factor leaves eq. (3.11) unchanged. One readily sees that condition (2.18) can be met for the quasi-particles with a sufficiently large N.

3.4. The INC and the (s > 1)-body distribution functions

Even if eq. (3.11) is a good equation, it does not provide any information on 2, 3,...-body distribution functions. They can be calculated by the INC cascades. They have a direct relationship with some observables. Let us mention the cluster distribution, which is presumably related to f_s ($s \geq 2$) at late

times of the collision only[50-52]). Other observables are linked with small relative momentum two-body distribution function : the deuteron yield, the two-proton interferometry yield, ... In these cases, the two-body distribution function does not seem to carry dynamical correlations. More interesting could be the large angle correlation yield, like the two-proton correlation yield at the quasi-free kinematics, as we discussed in section 4.5. This kind of information has not been exploited very much.

4. THE COLLISION DYNAMICS

4.1. Introduction

In this section, we will try to outline the main features of the dynamical evolution of the heavy ion system due to collisions. Roughly speaking, the system first evolves toward thermal equilibrium, but since it is not confined, it expands due to pressure work and disintegrates in many pieces. The collisions therefore determine the rate of equilibration, the rate of expansion and also the extension in phase space. We will discuss these points as well as the limiting situations which seem to hold for heavy systems. We will point out the importance of viscosity in some mechanism.

4.2. Evolution in phase space

Fig. 4.1. depicts the evolution in phase space as described by the lowest moments of the one-body distribution function

$$M_{ij} = \int d^3r d^3p\, \zeta_i \zeta_j f_1(\vec{r}, \vec{p}, t) , \qquad (4.1)$$

with ζ being the six-dimensional vector $\zeta = (\vec{r}, \vec{p})$. As can be seen, the compression of the system (especially in the longitudinal direction is accompanied by a tendency to thermalization (convergence of $\langle p_x^2 \rangle$ and $\langle p_z^2 \rangle$). The expansion is characterized by an increase of the $\vec{r}.\vec{p}$ correlations, which translate a continuous change from an adiabatic expansion to a free expansion. The thermalization is quite rapid, especially for the participants. However, it is not complete, essentially because of finite size effects. In other words, although the matter is stopped efficiently, some nucleons in the neighbourhood of the surface of the interaction zone can escape. The magnitude of this effect is of course dictated by the ratio of the mean free path

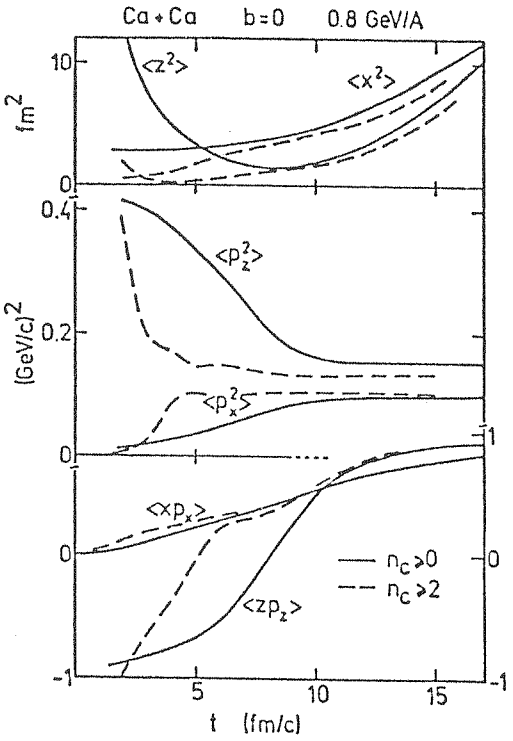

Fig. 4.1. *Evolution of the moments defined in eq. (4.1). The non-diagonal moments* $\langle xp_x \rangle$ *and* $\langle zp_z \rangle$ *are normalized by dividing them by* $(\langle x^2 \rangle \langle p_x^2 \rangle)^{1/2}$ *and* $(\langle z^2 \rangle \langle p_z^2 \rangle)^{1/2}$, *respectively. The full lines refer to all nucleons and the dotted lines to those nucleons having made at least two collisions. Adapted from the INC calculation of ref. 73).*

to the dimension of the system λ/R , which is of the order of 0.2 in the case of Fig. 4.1. The good stopping power of nuclear matter in the GeV/u range is largely due to inelastic effect (Δ production essentially), as was demonstrated in ref. [8].

The extension in phase space can be measured by the entropy per baryon. It is clear that the entropy is related to the thermalization process, i.e. due to collisions, but also to the equation of state. Indeed, if particle interaction is repulsive, less available energy will be thermalized for a given compression, since the available energy is fixed. It is not clear how to measure the entropy, but, if one adopts the d/p ratio, advocated by Siemens and Kapusta[50], or rather, refined methods[25,51], it is clear that the entropy is strongly affected by transparency effects[51,52].

The transparency has several consequences. Let us note the relatively small average number of collisions undergone by a nucleon[53] and the presence of quasi-free processes (see later).

4.3. Bulk dynamics

Except for transparency effects, it seems that the relaxation time is so short that perhaps the INC evolution does not depend so much upon the detail of the collisions and upon what happens on a very small scale (small scales are affected by a single collision, large scale average over many collisions) but rather, upon macroscopic variables. The INC would then approach the so-called bulk dynamics, which roughly corresponds to absence of surface and (small scale) mean free path effects. The simplest way to discuss that point is to consider the moments of the equation (3.11). We neglect the unnecessary complications due to the $\vec{\nabla}_p U$ term. The zeroth moment equation writes :

$$\frac{\partial \rho}{\partial t} + \vec{\nabla}.(\rho \bar{u}) = 0 \ , \tag{4.2}$$

where ρ is the density and where $\bar{u}$

$$\bar{u} = (m\rho)^{-1} \int d^3\vec{p}\ \vec{p} f_1(\vec{r}, \vec{p}, t) \tag{4.3}$$

can be interpreted as the collective velocity. The first moment equation can be written as

$$\rho \left[\frac{\partial \bar{u}}{\partial t} + \bar{u}.\vec{\nabla}\bar{u} \right] + \vec{\nabla}.\Pi = 0 \tag{4.4}$$

where the tensor Π is

$$\Pi_{ij} = S_{ij} + \delta_{ij} \mathcal{U}(\rho) \ , \tag{4.5}$$

with

$$\mathcal{U}(\rho) = \rho\, U - \int_0^\rho U(\rho')\, d\rho' \ , \tag{4.6}$$

and where the stress tensor $\mathbf{S}$ is defined by

$$S_{ij} = \int d^3p \, \delta p_i \delta p_j f_1(\vec{r}, \vec{p}, t) \ , \tag{4.7}$$

with $\frac{\delta\vec{p}}{m}$ being the deviation of the particle velocity from the collective velocity $\vec{u}$:

$$\vec{p} = m\vec{u} + \delta\vec{p} \ . \tag{4.8}$$

We have assumed the mean field depending upon ρ only, for simplicity. The second moment equation can be split into three equations

$$\left[\frac{\partial}{\partial t} + \vec{u}.\vec{\nabla}\right] R_{ij} + u_i \sum_k \nabla_k \Pi_{kj} + u_j \sum_k \nabla_k \Pi_{ki} = 0 \ , \tag{4.9}$$

$$\left[\frac{\partial}{\partial t} + \vec{u}.\vec{\nabla}\right] S_0 = -\frac{2}{3} S_0 \vec{\nabla}.\vec{u} - \frac{2}{3} \sum_i \sum_k \widetilde{S}_{ik} \nabla_k u_i - \vec{\nabla}.\vec{J}_Q \ , \tag{4.10}$$

$$\left[\frac{\partial}{\partial t} + \vec{u}.\vec{\nabla}\right] \widetilde{S}_{ij} = -S_0 \left[\vec{\nabla}.\vec{u}\right]_{ij} - \sum_k \left\{\widetilde{S}_{ik} \nabla_k u_j\right\}_{ij} - \sum_k \nabla_k \vec{J}_{\widetilde{S}_{ij}}$$

$$+ \int d^3p \left[\delta p_i \delta p_j - \frac{1}{3} (\delta\vec{p})^2 \delta_{ij}\right] \mathbb{I} \ , \tag{4.11}$$

where

$$R_{ij} = m^2 \rho \, u_i u_j$$

can be considered as the (local) collective flow tensor, and where

$$S_0 = \frac{1}{3} \mathrm{Tr}\, S \ , \quad S_{ij} = S_0 \delta_{ij} + \widetilde{S}_{ij} \ . \tag{4.12}$$

In eq. (4.11), $\mathbb{I}$ stands symbolically for the collision integral (r.h.s. of eq. (3.11)). We have also introduced the quantities

$$\vec{J}_Q = \int d^3p \, \frac{1}{3} (\delta\vec{p})^2 \vec{p} \, f_1(\vec{r}, \vec{p}, t) \ , \tag{4.13}$$

$$\vec{J}_{\widetilde{S}_{ij}} = \int d^3p \left[\delta p_i \delta p_j - \frac{1}{3} (\delta\vec{p})^2 \delta_{ij}\right] \vec{p} \, f_1(\vec{r}, \vec{p}, t) \ , \tag{4.14}$$

and the notation

$$\left[\vec{a}\,\vec{b}\right]_{ij} = a_i a_j - \frac{1}{3} \vec{a}.\vec{b} \, \delta_{ij} \ . \tag{4.15}$$

Eq. (4.9) is in fact trivially equivalent to the first moment equation. Eq. (4.11), as well as all the higher moment equations involve the collision integral $\mathbb{I}$. Only the five equations (4.2), (4.3) and (4.10) are independent of $\mathbb{I}$, which corresponds to conservation of particle number, momentum and energy by the collisions.

The moment equations form a hierarchy. The derivative of the n^{th} moment involves the $(n + 1)^{th}$ moment. The whole hierarchy is completely equivalent to the original equation (3.11). If one approaches the bulk dynamics, the lowest moments are sufficient to describe the evolution of the system. This is realized e.g. in the hydrodynamical limit. In the simplest case, called ideal fluid hydrodynamics, one assumes that the deviator $\widetilde{S}_{ij}$ is zero everywhere. The quantity S_0 , i.e. one third of the trace of $\mathbf{S}$, can then be identified with the pressure p . The hydrodynamical equations are then eq. (4.2), eq. (4.4) which becomes the Euler equation[54]

$$\rho\left[\frac{\partial}{\partial t} + \vec{u}.\vec{\nabla}\right] \vec{u} + \vec{\nabla} p = 0 \ , \tag{4.16}$$

and eq. (4.10), which is often written in term of temperature T (assuming $S_0 \simeq \frac{2}{3} c_v \rho T$ (for simplicity, valid for ideal gas), and no heat transport $\vec{J}_Q = 0$)

$$\left[\frac{\partial}{\partial t} + \vec{u}.\vec{\nabla}\right] T + \frac{T}{c_v} \vec{\nabla}.\vec{u} = 0 \ . \tag{4.17}$$

They have to be supplemented by the equation of state of the medium $p = p(\rho, T)$.

These equations have been used to study heavy ion collisions by several groups[55-63]. Some results are shown in Fig. 4.2 and compared with an INC calculation[24]. It is remarkable that, as far as the gross features are concerned, the two approaches yield very similar results. By looking carefully,

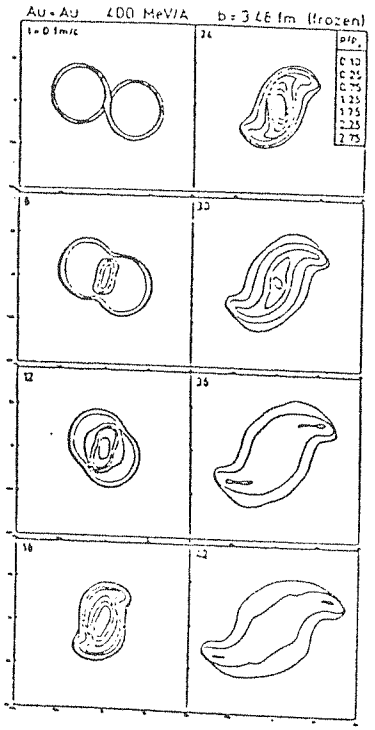

Fig. 4.2a. *Time evolution of the density as predicted by the INC calculation of ref. 24).*

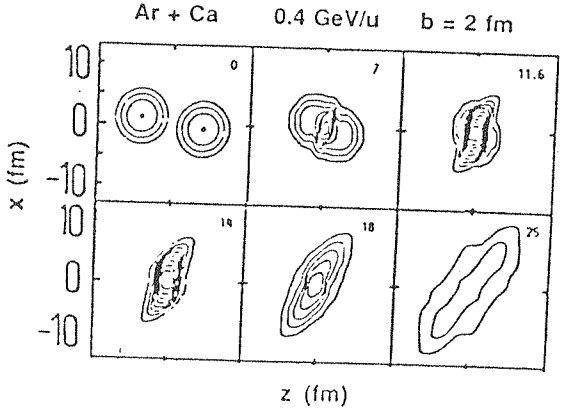

Fig. 4.2b. *Time evolution of the density as predicted by the hydrodynamical calculation of ref. 55). The ratio b/b_{max} is roughly the same as in part (a).*

one can detect some differences (time to achieve the maximum density, the value of the maximum density, the expansion rate,...). More subtile differences deal with the presence of spectators in the INC, correlations of particles (not observable in fig. 4.1), etc...

Actually, the numerical procedures used to solve the hydrodynamical equations seem to introduce some viscosity, an ingredient of a higher approximation, known as viscous fluid hydrodynamics. The latter is obtained by assuming the deviator $\tilde{S}_{ij}$ (and the heat current $\vec{J}_Q$) to be proportional to the gradient of $\vec{u}$ (T). We do not write down these equations. We only mention that they introduce[54] two parameters : the (shear) viscosity η and (less importantly in the nuclear case) the thermal conductivity κ.

Without entering into many details, it is clear that hydrodynamical equations are valid if the collision term vanishes. That does not imply a collisionless regime. On the contrary, that demands so efficient collisions that the deviator (and consequently the last term in eq. (4.11)) vanishes in an extremely short time : this is the short relaxation time limit.

The long relaxation time limit, which is discussed in refs. [53,64] may also be of some interest for nuclear physics, but at very small excitation energy.

To illustrate somewhat more the collision dynamics, it is interesting to look at its limit of small perturbations. The latter is obtained by taking a small departure from an equilibrium situation. The static solutions of eq. (3.11) for an infinite medium has the form $f_1^{(0)}(\vec{p})$, which would reduce to the Fermi-Dirac distribution if there were no mean field U. One can look for small perturbations from this static solution

$$f_1(\vec{r}, \vec{p}, t) = f_1^{(0)}(\vec{p}) + \delta f \qquad (4.18)$$

with

$$\delta f = a \exp[i(\vec{k}.\vec{r} - \Lambda t)] \qquad (4.19)$$

and determine the frequencies Λ by linearizing the transport equation (3.11). This is done in great detail in ref. [29]. We only quote the results here. Their are five eigenvalues (modes), which are the same as the ones that are obtained by studying small perturbations on the hydrodynamical equations. They are listed in the Table below. In addition, this approach provides microscopic expressions for the transport coefficients (in second order in the wave number k). In conclusion, the collision dynamics is the response due to collisions of the system to (small or large) perturbations of density, current and

temperature. The heat conductivity is however negligible in nuclear system.

Table : Normal modes of eq. (3.11)

Λ	Denomination
$\Lambda_1 = ic_s k - \frac{1}{2\rho}\left[\left(\frac{1}{c_v} - \frac{1}{c_p}\right)\kappa + \frac{4}{3}\eta + \zeta\right]k^2$	sound mode
$\Lambda_2 = -ic_s k - \frac{1}{2\rho}\left[\left(\frac{1}{c_v} - \frac{1}{c_p}\right)\kappa + \frac{4}{3}\eta + \zeta\right]k^2$	sound mode
$\Lambda_3 = -\frac{\eta}{\rho}k^2$	shear mode
$\Lambda_4 = -\frac{\eta}{\rho}k^2$	shear mode
$\Lambda_5 = -\frac{\kappa}{\rho c_p}k^2$	thermal mode
Remark : $c_S = (\partial p/\partial \rho)_S^{1/2}$ is the sound velocity.	

4.4. Scaling properties

We want here to discuss a question raised in ref. [65], namely to know how to determine whether the bulk dynamics is realized. This may be studied by looking at scaling properties of some observables, as was suggested in ref. [66]. In this context, the use of similarity theory[54,67] has been shown (for the first time in ref. [65]) to be very powerful. We will closely follow the presentation of this work.

Let us start with ideal fluid hydrodynamics (eqs. (4.2), (4.16) and (4.17)). They possess a remarkable property. Let us call $\phi(\vec{r}, t)$ any field entering these equations ($\phi = \rho$, $\vec{u}$ or T). If $\phi(\vec{r}, t)$ is a solution, $\phi(\Lambda\vec{r}, \Lambda t)$ is also a solution, provided of course that the initial conditions are scaled in the same way. This is of course realized if one goes from a system, say Ca + Ca, to a larger system, Au + Au e.g. at the same incident energy and the same impact parameter over radius ratio. (The correspondence will be obtained by scaling

the time in the same way). This scaling law is known in similarity theory[67] as dictated by the Strouhal number

$$[S] = \left[\frac{u\tau}{R}\right] \qquad (4.20)$$

where u, R and τ are the characteristic velocity, length and time of the system. Here, τ is proportional to R[65]. The similarity theory tells that any dimensionless quantity ψ is a function of [S] only. However, if one concentrates on a given impact parameter, another dimensionless geometrical parameter b/b_{max} has to be introduced :

$$\psi = \psi([S], b/b_{max}) \ . \qquad (4.21)$$

A result like this was presented in ref. [66] for the inclusive spectra, but assuming some normalization proportional to the system (and summation over b). In ref. [65] the emphasis was put on ψ characterizing the flow properties. The latter are embodied by the so-called sphericity (or flow) tensor

$$Q_{ij} = \lim_{t\to\infty} \int d^3r\, p_i p_j f(\vec{r}, \vec{p}, t) = \lim_{t\to\infty} \int d^3r\,(R_{ij} + S_{ij}) \ . \qquad (4.22)$$

Particular attention was drawn to the so-called flow angle[68], which is the angle Θ of axis of this ellipsoid ($Q_{ij} = Q_{ji}$ and positive definite) with respect to the incident beam. It was argued that (see fig. 4.2) the pressure build in during the compression stage pushes the spectator zone apart. This is demonstrated by eq. (4.9), which tells that the variation of R_{ij} is due basically to (see eq. (4.5) and ref. [24]) $\nabla_i p$ and $\nabla_j p$. The average flow angle would then have property (4.21) and would be the same for all symmetric systems. The value of Θ may depend upon the dynamics, however. If, as suspected, the dynamics is closer to viscous fluid dynamics, any dimensionless physical quantity can be expressed as

$$\psi = \psi\left([S], [\mathcal{R}], \frac{b}{b_{max}}\right) \ , \qquad (4.23)$$

where $[\mathcal{R}]$ is the Reynolds number[54] defined as

$$[\mathcal{R}] = \left[\frac{u\,\rho\,R}{\eta}\right] \ . \qquad (4.24)$$

In ref. [65], it was shown that the dependence upon the Reynolds number is non negligible. A rough estimate gives ($b \lesssim b_{max}/2$)

$$\tan\langle\Theta\rangle \approx \left\{[S]\left(1 - \frac{b}{b_{max}}\right) - \frac{3}{[\mathcal{R}]}\right\}\frac{\bar{\varepsilon}}{3\,\bar{\varepsilon}_z}\,, \qquad (4.25)$$

where $\bar{\varepsilon}$ and $\bar{\varepsilon}_z$ are the average energy and average energy in the z-direction respectively, of the nucleons participating to the flow (it is roughly equal to the aspect ratio q [9]). Relation (4.25) is compared to experimental data at 400 MeV/A in Fig. 4.3 (using $q \approx 1.5$). The correspondence gives $[\mathcal{R}] \approx 8$ for Nb + Nb, which is very close to the free gas value[69] at this energy. We recall that the viscosity parameter η is related to the cross-section.

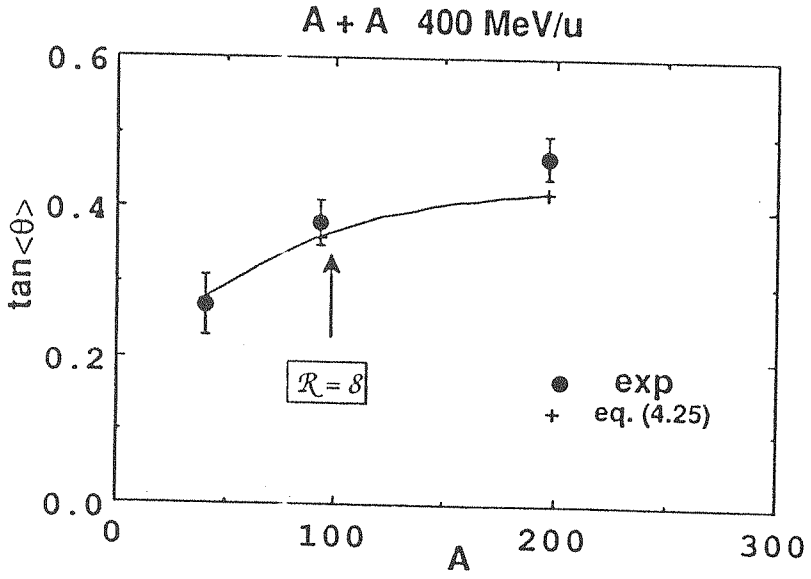

Fig. 4.3. *Comparison of the flow angle (dots), measured in ref. [68], with formula (4.25) (full line), using a Reynolds number (eq. (4.24)) $[\mathcal{R}] = 8$ for Nb + Nb.*

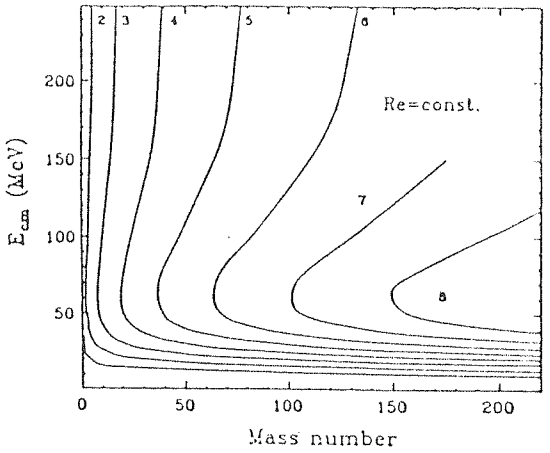

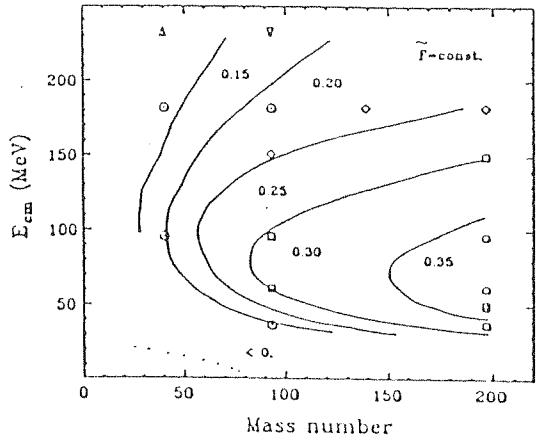

Fig. 4.4. *Above : lines of constant Reynolds number (values given by the numbers), as evaluated in ref. [69]. Below : lines of constant $\tilde{F}$ (eq. (4.26)) as extracted from experiment (symbols). Adapted from ref. [70].*

A more extensive analysis was done recently[70], not only on the flow properties, but also on other quantities, like the pion and γ cross-sections. In Fig. 4.4, we present some of the results of ref. [70]. There is a remarkable resemblance between the dimensionless transverse momentum

$$\tilde{F} = \frac{d\langle p_x \rangle}{dy} , \qquad (4.26)$$

another dimensionless quantity related to the flow and defined in ref. [71] and the value of the Reynolds number calculated with a viscosity coefficient as evaluated in ref. [69]. This strongly suggests that the flow properties are much more sensitive to viscosity than to equation of state. However the quoted value of Reynolds number refer to small density, which may be not so relevant (see Fig. 4.2). This important result nevertheless deserves more attention.

4.5. Deviation from bulk properties

Several facts point to departures from bulk dynamics. For instance, the entropy per particle seems to change significantly with impact parameter[52], which indicates λ/R effect. The most striking and well-known effect is the

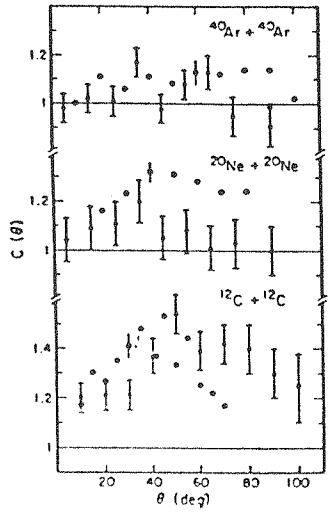

Fig. 4.5. *Variation of the two-proton correlation factor (see ref. [72]) as a function of the relative angle θ. The maximum corresponds to the quasi-free scattering kinematics. The heavy dots are the experimental data (ref. [72]) and the small dots indicate the INC calculations of ref. [9].*

observation of two-proton correlations at quasi-free kinematics, typical of knock-out process. These correlations were studied experimentally in ref [72] and reproduced by INC calculations as shown in Fig. 4.5. The importance of the knock-out process disappears for large systems. Detailed analysis of these and other features indicate that bulk dynamics is approached in central collisions of large systems, corresponding to large multiplicity events.

5. COMPARISON WITH EXPERIMENT

5.1. Introduction

As it is impossible to review the numerous existing results, we shall only point out the most important ones. In doing so, one must keep in mind that several INC models have been used, which differ either by their basic assumptions (see section 2), or by some "details" which can affect the observables. Reviews of the models can be found in refs. [2,73,74]. Furthermore, due to successive improvements, or to the use by different groups, several versions of each model appeared. Therefore, only common trends can be related to INC in general. When dealing with accurate and quantitative results, the model and its version have to be mentioned. We shall restrict ourselves to the observables related to the participant nucleons (i.e. the nucleons who suffered a large momentum transfer during the reaction). Indeed, the purpose of the cascade models is not to describe the spectators physics, as the latter is dominated by soft collisions. We shall not discuss either the composite (d, t, He, ...) yields as they are not predicted by the cascade alone. The latter should then be supplemented by another model such as coalescence, evaporation, "pre-equilibrium effects", etc... Description of composite production (and related entropy evaluation) can be found in refs. [25,74-84]. Besides, the strange particle production (mainly K's) is also beyond the scope of this paper, as the calculations are performed only as a perturbation to the pure cascade process[85,86]. Finally, as we shall not come to this point later, let us mention INC studies of the shape and size of the participant "fireball" as a function of time in order to calculate interferometry[87,88] or Coulomb[89] effects.

We shall first present proton and pion spectra, and then go to nucleon-nucleon correlations. Due to their expected connection with nuclear equation of state, pion multiplicity and observables related to the flow and stopping power of nuclear matter have been calculated by many authors.

5.2. Nucleon spectra

Fig. 5.1 displays the inclusive proton spectra from the first version of the Liège cascade[2] in comparison with experiment for Ar + Ar at E/A = 800 MeV. As the cascade does not predict the composite yields, the experimental data represent the "proton-like" cross-section (eq. (2.13)). We can see that the

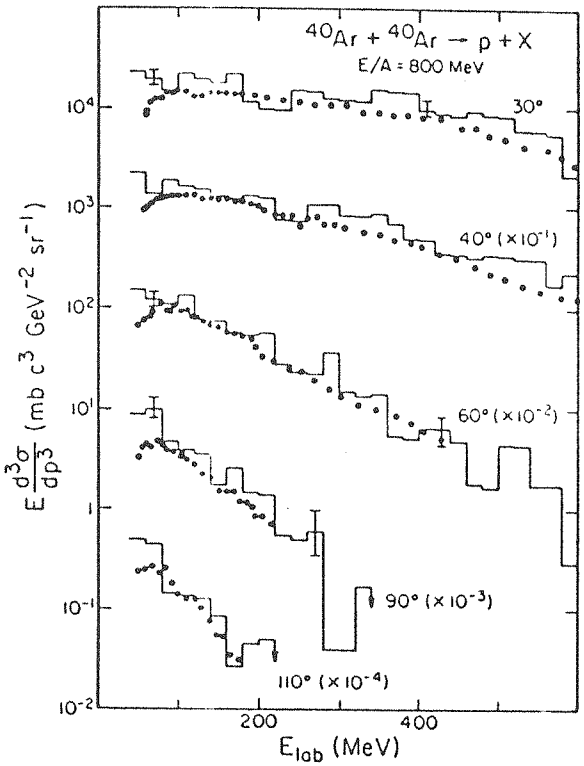

Fig. 5.1. *Invariant proton inclusive cross-section as a function of the proton laboratory kinetic energy for the Ar + Ar system at the incident energy E/A = 800 MeV. Five laboratory emission angles have been selected. The histograms are the results of the Liège cascade, and the dots give the experimental data from ref. 90), for Ar + KCl.*

agreement is quite good. Notice however the logarithmic scale : the discrepancies are less than say, ~ ± 40 %. At low energy, the model overestimates the data, but this can be accounted for by the expected inability of the cascade to describe the (target) spectators or quasi-spectators. For smaller angles, the model overestimates slightly the data. Similar trends are observed for C + C and Ne + Ne reactions. The inclusive proton c.m. angular

distribution for the reaction Ar + Ar at E/A = 800 MeV are fairly well reproduced for a proton c.m. energy of 200 and 400 MeV, while, for 600 MeV it is slightly too forward and backward peaked. To our knowledge, the results of the Liège cascade[9] have not been compared to experimental inclusive proton spectra, neither for the improved versions of the code (which includes a better description of the pion and delta dynamics, of the nucleons's binding in the initial nuclei and in the spectator pieces, and of the elementary cross-sections (charge dependence) ; for description and discussion of those successive improvements, see refs. [24,91,92]), nor for other systems than those quoted above (except Ne + Na F at E/A = 400, 800, 2100 MeV in refs. [85] and [8]). Indeed it would be interesting to study the energy dependence and to go to heavier systems. Preliminary results seem to indicate that for heavy symmetric systems, some discrepancies with the experimental data are found at rather small laboratory angles[93]. In ref. [24], it is shown that the proton spectra can be modified by using a particular prescription to simulate nucleon binding ("freezing").

Inclusive proton spectra have been calculated by different authors, using different codes, mainly for light projectiles (A_P = 1 to 40), for a large variety of targets (A_T = 12 to 238), and for energies ranging from E/A = 0.25 GeV to 2.1 GeV. In general, the quality of the agreement between the calculations and the data is comparable to what is shown on Fig. 5.1. The comparison of the first version of the Yariv and Fraenkel cascade with the experimental data favours the so-called "slow rearrangement" prescription[17]. The second version[18] (including cascade-cascade collisions, see section 2.3) has been used for calculating low energy proton spectra for Ne + U at E/A = 400 MeV and Ar + Ca at E/A = 1050 MeV. At rather large angles and energies, the agreement with the data is satisfactory, while once again a discrepancy occurs at the lowest proton laboratory energy ; but here, the yield is underestimated probably because the binding prescription is not associated with an evaporation one. The Stevenson cascade[10] provides also a rather good agreement with experimental inclusive proton spectra (from ~ 50 to 200 MeV) for He and Ne + U collisions at E/A = 250 and 400 MeV. For Ne + Na F (E/A = 800 MeV) reactions, the high energy proton cross-section at small laboratory angles are overestimated as for Ar + Ar using the Liège cascade. Let us quote also the comparison of neutron to proton spectra in ref. [94]. At low laboratory angles (≤ 90°), the Toneev and Gudima cascade[80] predicts a steeper decrease of the invariant proton inclusive cross-section (as a function of proton energy in the range ~ 50 to 350 MeV) than what is observed experimentally, while the agreement is quite good at larger angles. Let us also quote the comparison with the Dubna experimental data in refs. [95,96], at energies (till ~ 4 GeV/u) larger than the Bevalac ones (~ 0.2-2.1 GeV/u). Finally, let us

mention the predictions of the Kitazoe et al. cascade model[13,97,98] which are in rather good agreement with the experimental data for Ne + Na F (E/A = 800 MeV ; ~ 0.5-3.0 GeV/c protons) and Ne + U (E/A = 393 MeV ; ~ 50-200 MeV protons).

Comparison with experimental proton spectra measured in correlation with multiplicity cuts (assumed to correspond to impact parameter cuts[99]) is of particular interest because discrepancies due to compression effects are expected to be larger for central collisions. To our knowledge, only few comparisons have been made. For the reactions Ar + Ar and Ar + Pb at E/A = 800 MeV, the Yariv and Fraenkel cascade[17] do not show any large discrepancy in what concerns proton angular distributions. For the reaction Ne + U at E/A = 393 MeV, the experimental low energy proton angular distribution show a "forward suppression" when triggering on high multiplicity events. The "forward peaking" exhibited by the Yariv and Fraenkel and the Stevenson cascades has been presented as a first indication that the cascade lacks the hydrodynamic-like "collective flow" of nuclear matter[100,101]. Note that there can also be an influence of binding and Fermi motion prescriptions, composite formation or Coulomb effect on those low energy proton spectra. In ref. 97), Kitazoe et al. show that including a Pauli blocking prescription depletes the forward peaking. See also the discussion of ref. 80).

5.3. Pion spectra

Pion production is put in the INC through the inelastic channels of the NN interaction. In most cases, at least the reactions $NN \rightleftarrows N\Delta$ are simulated, but the models can differ in the way deltas and pions are described during the collision. Fig. 5.2 shows the pion inclusive spectra predicted by the first version of the Liège cascade[9] for the reaction Ar + Ar at 800 MeV/u. The total yield is overestimated (see section 5.5) while the shape of the spectra is close to the experimental one for large emission angles, but not steep enough at forward angles. The spectra for Ne + Na F collisions have also been calculated[8,85], showing a better agreement with the data for high incident energies. The crude assumptions made in the first version of the code (zero width of the delta mass distribution, no $\Delta \rightleftarrows N\pi$ reaction allowed) were subsequently eliminated[3,91], but no systematic comparison of the new version with inclusive spectra has been made. The π^- spectra measured in Ar + KCl (E/A = 1.8 GeV) central collisions have been also compared to the Liège cascade results[102]. The model predicts a too large anisotropy for medium

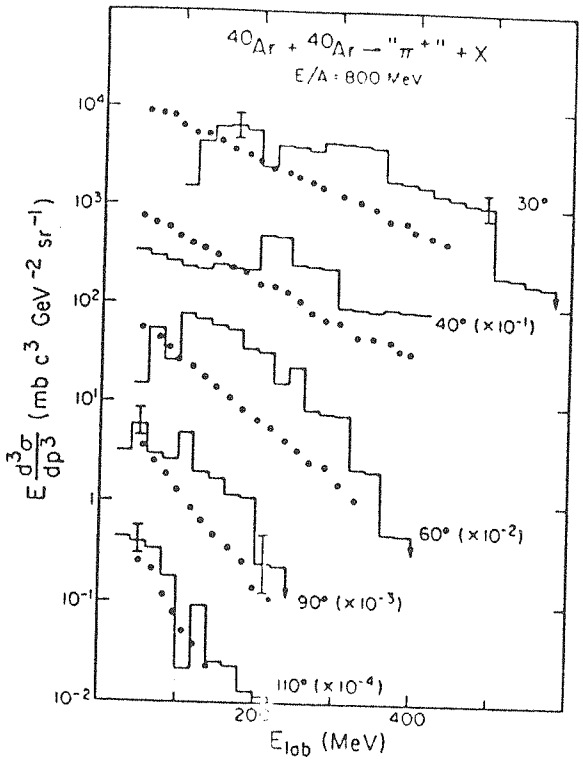

Fig. 5.2. *Invariant pion inclusive cross-section as a function of the pion laboratory kinetic energy for the Ar + Ar system at 800 MeV per nucleon. The histograms are the results of the Liège cascade[9]) and the dots represent the experimental data of ref. 90).*

and large pion energies, but the shape of the 90° c.m. spectrum is correctly reproduced except for a 5 % high energy component.

The first version of the Yariv and Fraenkel cascade[17] also overpredicts the pion yield, but the shape of the spectra is closer to experiment. Their second version compares moderately well with inclusive low energy pion data for the Ar + Ca (E/A = 1.05 GeV) reaction. However the model predicts an experimentally observed bump of the invariant cross-section in the region $y_{c.m.} = 0$, but at a transverse momentum of ~ 100 MeV/c instead of the experimental ~ 50 MeV/c. The Gudima and Toneev cascade[80] gives a good agreement with the experimental inclusive π^- spectra for the reaction Ar + KCl at 800 MeV/u. A rather good agreement is also found at E/A = 2.1 GeV[85,96] and at Dubna energies[103,104]. The Kitazoe et al. cascade[13,98] gives an amazing agreement with the experimental Ar + KCl and Ne + Na F data, which is due, according to the authors, to their improved description of π's and Δ's and to their binding prescription.

5.4. Proton-proton correlations

The study of the two proton correlations is of particular interest because they can be related to quasi-free nucleon-nucleon elastic scattering ("knock-out" process), and also to the absence of cylindrical symmetry of the initial state (correlations related to the "bounce-off", "side-splash", or spectators shadowing, etc...). In the first case, the magnitude of the correlation can be related to the degree of equilibration reached, and in the second case to the collective behaviour of nuclear matter. Of course, other causes for two proton correlations can be considered. The correlation coefficient measured for C + C, Ne + NaF and Ar + KCl at E/A = 800 Mev [90] exhibits a broad peak that can be accounted for by knock-out nucleons and that progressively flattens when the mass of the system increases. The Liège cascade reproduces this trend (see Fig. 4.5), but the peak is slightly shifted, while the magnitude of the correlation is roughly accounted for. It is interesting to notice that the first version [17] of the Yariv and Fraenkel cascade overestimates the quasi-elastic peak for C + C, while the second one [18] (which allows cascading nucleons reinteractions), achieves a better agreement.

5.5. Pion yield

The pion multiplicity, or the pion production cross-section (the mean of the former is just equal to the latter divided by the total reaction cross-section) gave rise to many calculations, partly because it was once suggested [105] that the mean pion multiplicity could be considered as a "nuclear matter thermometer" from which the fractions of the total available energy corresponding to kinetic and to potential energy could be estimated. In such a picture, the cascade models should predict too many pions because they do not involve the repulsive potential energy due to compression. Fig. 5.3 shows the predictions of the second version of the Liège cascade [3,91] (i.e. in which the Δ has a non-zero width, and the reactions $\Delta \rightleftarrows N\pi$ are allowed ; the results are represented by a continuous line with open circles) together with experimental results [106] (dashed line) for central Ar + KCl collisions. Actually, the model overpredicts the pion multiplicity by ~ 1.5 units. A similar result is obtained using the Yariv and Fraenkel cascade [107]. The Gudima and Toneev cascade [80] also predicts too large pion multiplicities for Ar + KCl (E/A = 1.8 GeV) reactions, but the linear dependence $<n(\pi^-)> \propto Q$ (where Q is the participant proton number) is nicely reproduced. The width of the pion multiplicity distribution is also correctly predicted. Finally, let us quote the

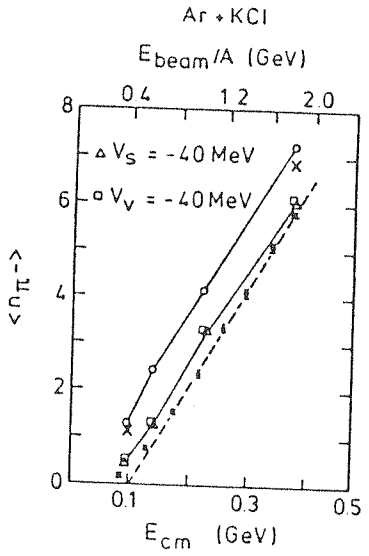

Fig. 5.3. *Mean π^- multiplicity in central Ar + KCl reactions, as a function of the c.m. incident energy. The experimental data [106] correspond to full dots and dashed line. The Liège cascade results [3,91] are represented by open circles and continuous line. The open squares and triangles along the second continuous line correspond to two binding energy prescriptions where the nucleons suddenly loose 40 MeV at their first collision [91].*

La + La results : for central collisions, the Liège cascade predicts ~ 5 more π^- than what is measured, for experimental mean π^- multiplicities [108], ranging from ~ 4 to ~ 15, corresponding to low and high multiplicity events, respectively.

As can be seen in Fig. 5.3, including a binding energy prescription strongly improves the agreement with the data. The reason for that is very simple : in the Liège cascade, the system has too large an energy in the initial state because the nucleons have a Fermi motion without being bound in the nuclei. As the N-N pion production cross-section increases with the relative N-N kinetic energy, one can expect too many pions ; while reducing this kinetic energy through a binding energy prescription will decrease the pion multiplicity. Notice however that both the Yariv and Fraenkel cascade, and the Gudima and Toneev one take into account the potential well of the two initial nuclei ; but in a different way than what is done in the Liège cascade. The Kitazoe et al. cascade reproduces fairly well the experimental Ar + KCl mean pion multiplicities [13,97]. The authors showed that their binding energy prescription also leads to a lower pion yield, but they discuss other reasons [13] for the difference with the Liège results. The question of the binding prescription has been recently reexamined by Medeiros et al. [109] who find

also a good agreement with the data using a new prescription. In ref. [110], the π^+ and π^- multiplicities calculated from the Liège cascade have been compared to the data for the ^{4}He + A (E/A = 800 MeV) reactions, using an improved version of the model (isospin dependence of the elementary cross-sections, "freezing", binding energy prescription, and improved Pauli blocking). For heavy targets and high proton multiplicity reactions, even this improved version of the code still strongly overpredicts the data suggesting that pion absorption in nuclear matter could be underestimated in the model. As a matter of fact, the medium effects can strongly modify the N, Δ, π dynamics[91,92,11,8,111,112]. In ref. [11], it is shown that a good agreement with the experimental Ar + KCl data can be achieved by slightly shifting the delta mass, or by decreasing the inelastic cross-section. The pion yield in p + A reactions is overestimated by the standard Liège cascade, and the true pion absorption in π + A is underestimated. Those discrepancies can be removed by strongly increasing the in-medium pion absorption[11,92]. Finally, let us quote pion yield calculations at the Dubna energies (E/A = 3.4-3.7 GeV) : only for heavy targets and central collisions, the cascade models tend to predict too many pions[103,104,113-115].

5.6. Global variables and collective flow of nuclear matter

The cascade predictions have been also examined for the observables obtained from exclusive (or quasi-exclusive) measurements. Such observables are generally studied in correlation with an impact parameter selection. Experimentally, the selection is made on the charged particle multiplicity. Note that only few comparisons have been made with experimental multiplicity distributions. In ref. [17], a rather good agreement is obtained with Ne + Au experimental multiplicity distribution. In refs. [116,117], the isotropy of Ar + Pb high multiplicity events is calculated using the Liège cascade, in comparison with experimental data. They find that the cascade events are more forward peaked than the experimental ones, which could be due to a too low stopping power of nuclear matter in the model. In order to study the collective flow of nuclear matter[118], the sphericity tensor (eq. (4.22)) was measured, and also calculated using cascade models[80,24,99,119-123]. From the sphericity tensor, an angle with respect to the beam axis called flow angle can be determined for each collision. The flow angle gives the average emission direction of the flowing nuclear matter. The flow angle distribution was first measured for Ar + Pb [116] and Ca + Ca or Nb + Nb [68]. In the first case, the results were compared to the Liège cascade predictions, and in the

second case to the Yariv and Fraenkel cascade ones. In both cases, the models predict too low flow angles. This can be accounted for by the lack of compression energy in the cascade. Contrarily to an erroneous statement, the cascade models generally predict a non-zero flow. It has been demonstrated in ref. [24] that the Liège cascade predicts a finite flow, but that its magnitude is lower than the experimental one. A quantitative evaluation of the discrepancy is difficult because of the uncertainties due to the experimental filter ; and also because, once again, the way the binding of the nucleons and the Pauli blocking are treated influences the final flow angle values[122,123]. The Kitazoe cascade[123] predicts rather large flow angles, close to experimental ones, presumably (at least partly) because of the choice of the binding prescription. Note that a more satisfactory way to include the binding potential consists in putting in a locally calculated mean field as in VUU, BUU or "Landau-Vlassov" models (see section 6).

Another method for flow measurement was proposed by Danielewicz and Odyniec[71], which consists in using the $\langle p^x \rangle$ versus y function (see eq. (4.26)), y being the rapidity of the nucleons and $\langle p^x \rangle$ the mean value of their transverse momentum projected on the (reconstructed) reaction plane. In their paper, Danielewicz and Odyniec showed that the Liège cascade exhibits a finite flow smaller than the experimental one. Fig. 5.4 shows the experimental

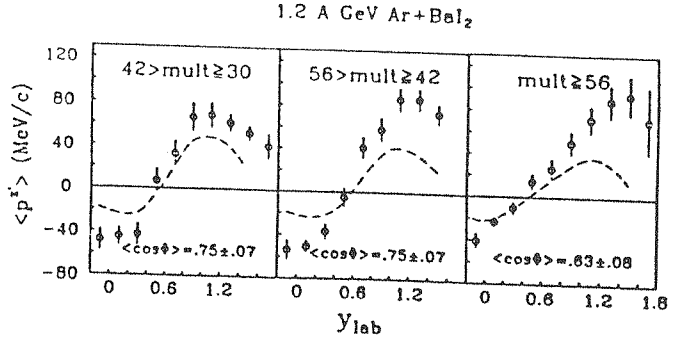

Fig. 5.4. *Mean transverse momentum per nucleon projected on the reaction plane as a function of rapidity. The circles correspond to the experimental Ar + BaI_2 results for three multiplicity cuts. The dashed curves give the results for the INC model of ref. [8] with a freezing prescription. The quantity ϕ is the estimated azimuthal angle with respect to the reconstructed[71] reaction plane. Adapted from ref. [128].*

results for (A_p = 40) + (A_T ~ 132) reactions together with the Liège cascade results. Zero flow would correspond to $\langle p^x \rangle = 0$ for all rapidities. Once again, the INC predicts an appreciable amount of flow, but smaller than the experimental one. Such a statement seems to hold for several models, several target-projectile masses and several incident energies[24,116,68,71,124-126], including Dubna energies[127].

6. PERSPECTIVES

6.1. Possible improvements of the INC

As we have seen, some results of the codes can be sensitive to the way the following physical effects are simulated : (i) binding of the nucleons in the two initial nuclei, and in the subsequent spectator pieces ; (ii) description of the initial nuclei (density profile, Fermi momentum distribution, Pauli correlations) ; (iii) taking account of the composite production and of the particles evaporation from the spectator pieces ; (iv) Pauli blocking simulations during the collision ; (v) isospin dependence of the elementary cross-section ; (vi) description of the inelastic channels (non resonant π production, inclusion of several baryonic resonances) ; (vii) description of the delta mass distribution. Hence, a first type of improvements consists in simulating as carefully as possible the different physical effects mentioned above. The last version of the Liège cascade which has been compared to He + A [110], p + A, A + A and π + A [11] reactions includes the isospin dependence of elementary cross-sections, the Pauli blocking governed by local phase space density, the binding potential and the "freezing" of spectators.

6.2. Mean field theories

However, despite of these improvements, the cascade *stricto sensu* (i.e. a model using straight line trajectories in between the collisions) lacks an important effect, which has received much attention these last three years, namely the time-dependent local mean field, as introduced in eq. (3.11). New methods, devised to cope with this difficulty, named VUU, BUU or "Landau-Vlassov" have appeared. In these methods (some of them are described in this book), each nucleon follows a curved trajectory, calculated by Newtonian mechanics, subject to the acceleration due to the gradient of a scalar field $U(\rho(\vec{r}))$, where ρ is the density in configuration space. As for the collisions, the method is largely, if not totally, taken from the cascade. The field U is then calculated self-consistently from the actual density distribution. These methods establish a connection with the equation of state. The ultimate goal is to extract the equation of state from the comparison of predictions with experiment. However, before any conclusion can be drawn with some confidence, several questions have still to be answered. We list here the most important ones (still keeping with a theory using baryons and mesons as basic Schrödinger particles) : (a) what is the importance of the quantum effect in collisions (see section 3.2) ? ; (b) how to treat correctly the production mechanism ? ; (c) how important are the medium effects ?

6.3. Beyond eq. (3.11) and the one-body distribution function

Much emphasis is presently put on eq. (3.11) and the one-body distribution function. However, as we said in section 2, the INC is potentially able to study high-order distribution functions. This may be used to study two general questions : (a) high-order distribution functions should be related to many-body correlations, responsible for the appearance of fragments ; (b) high-order distribution functions are related to fluctuations of lower-order distribution functions or of lower-order observables (see section 2). The first question has not been studied by dynamical simulation, like INC, up to now, except for large angle p-p correlations (see section 4.5). The second question has been investigated for the case of the flow angle only (as far as we know), for which the correlations seem rather trivially related to the number of particles. We believe, however, that it would be worthwhile to pursue the use of simulation methods to study these two (and perhaps other) problems.

7. CONCLUSION

The INC model has been very successful in explaining the main features of the experimental data for heavy ion collisions in the GeV/u range. Furthermore, this model has been very helpful in three respects : (a) it first gave an elaborate picture of phase space evolution of the system ; (b) it contributed to promote simulation methods as a powerful tool of investigation in nuclear physics ; (c) it made possible the study of collision dynamics in situations far from equilibrium. Presently, the INC *stricto sensu* is progressively replaced by mean field theories, which to some extent, are generalizations of the INC approach.

The INC, owing to its simplicity due to the use of straight line trajectories, can still be of great help in situations where the mean field effects are not important or where they can be handled very simply, or where the production

processes are important. We think especially to hadron-nucleus or antibaryon-nucleus interactions, especially in the 1 to 10 GeV range. However, we think that an effort should be done in the next future to improve the collision dynamics : introduction of quantum effects in collisions, improvement of the crude production models, medium corrections.

Finally, we recall that the simulation method used in INC, in contradistinction with the quasi-particle methods used in mean field theories, is a good tool to evaluate high-order distribution functions as well as fluctuations, in spite of the problems for achieving sufficient statistics.

Acknowledgements : We are very grateful to the members of the Centre Culturel de Coo (CCC) for their repeated encouragement.

REFERENCES

1. R. Serber, Phys.Rev. **72**(1947)1114.
2. J. Cugnon, Nucl.Phys. **A387**(1982)191c.
3. J. Cugnon, D. Kinet and J. Vandermeulen, Nucl.Phys. **A379**(1982)553.
4. K.K. Gudima and V.D. Toneev, Sov.J.Nucl.Phys. **27**(1978)351.
5. K.K. Gudima, H. Iew and V.D. Toneev, J.Phys. **G5**(1978)229.
6. J.P. Bondorf, H.T. Feldmeier, S. Garpman and E.C. Halbert, Z.Phys. **279**(1976)385.
7. E.C. Halbert, Phys.Rev. **C23**(1981)295.
8. J. Cugnon, T. Mizutani and J. Vandermeulen, Nucl.Phys. **A352**(1981)505.
9. J. Cugnon, Phys.Rev. **C22**(1980)1885.
10. J.D. Stevenson, Phys.Rev.Lett. **41**(1978)1702.
11. J. Cugnon and M.-C. Lemaire, Nucl.Phys. **A489**(1988)781.
12. H.W. Barz and H. Iwe, Phys.Lett. **143B**(1984)55.
13. Y. Kitazoe et al., Phys.Lett. **B166**(1986)55.
14. P. Jasselette, J. Cugnon and J. Vandermeulen,Nucl.Phys.**A484**(1988)542.
15. G.D. Harp, Phys.Rev. **C10**(1974)2387.
16. M. Blann, Ann.Rev.Nucl.Sci. **25**(1975)123.
17. Y. Yariv and Z. Fraenkel, Phys.Rev. **C20**(1979)2227.
18. Y. Yariv and Z. Fraenkel, Phys.Rev. **C24**(1981)488.
19. H.W. Bertini et al., Phys.Rev. **C14**(1976)590.
20. K. Chen et al., Phys.Rev. **166**(1968)949.
21. N. Metropolis et al., Phys.Rev. **110**(1958)185.
22. M.R. Clover, R.M. De Vries, N.J. DiGiacomo and Y. Yariv, Phys.Rev. **C26** (1982)2138.
23. A.S. Iljinov, V.I. Nazaruk and S.E. Chigrinov, Nucl.Phys. **A382**(1982)378.
24. J. Cugnon and D. L'Hôte, Nucl.Phys. **A452**(1986)738.

25. G. Bertsch and J. Cugnon, Phys.Rev. **C24**(1981)2514.
26. A.R. Bodmer and C.N. Panos, Nucl.Phys. **A356**(1981)517.
27. L. Wilets, E.M. Henley and A.D. Mac Kellar, Nucl.Phys. **A282**(1977)361.
28. S.E. Koonin, Phys.Lett. **B70**(1977)43.
29. R. Balescu, "Equilibrium and Nonequilibrium Statistical Mechanics", J. Wiley, New York (1975), p. 98.
30. R.F. Snider, J.Chem.Phys. **32**(1960)1051.
31. M.W. Thomas and R.F. Snider, J.Stat.Phys. **2**(1970)61.
32. L. Waldmann, Z.Naturforsch. **13a**(1958)609.
33. W. Botermans and R. Malfliet, Phys.Lett. **B171**(1986)22.
34. J. Cugnon, A. Lejeune and P. Grangé, Phys.Rev. **C35**(1987)861.
35. L.P. Kadanoff and G. Baym, "Quantum Statistical Mechanics", W.A.Benjamin, New York (1962).
36. P. Danielewicz, Ann.Phys. (N.Y.) **152**(1984)239.
37. P. Danielewicz, Ann.Phys. (N.Y.) **152**(1984)305.
38. J.-P. Jeukenne, A. Lejeune and C. Mahaux, Phys.Rep. **25C**(1976)85.
39. G. Bertsch, H. Kruse and S. Das Gupta, Phys.Rev. **C29**(1984)673.
40. H. Kruse, B.V. Jacak and H. Stöcker, Phys.Rev.Lett. **54**(1985)284.
41. J.J. Molitoris and H. Stöcker, Phys.Rev. **C32**(1985)346.
42. J. Aichelin et al., J. de Physique **C2**(1987)165.
43. A. Bonasera et al., Catania Univ. preprint (1989).
44. W. Cassing et al., Phys.Lett. **B181**(1986)217.
45. C. Grégoire et al., Nucl.Phys. **A447**(1985)55c.
46. C. Grégoire et al., Nucl.Phys. **A465**(1987)317.
47. V.E. Bunakov and G.V. Matvejev, Z.Phys. **A322**(1985)511.
48. K. Binder (ed.), "Monte-Carlo Methods in Statistical Physics", Springer, Berlin (1975).
49. E. Suraud et al., private communication.
50. P.J. Siemens and J.I. Kapusta, Phys.Rev.Lett. **43**(1979)1486.
51. H.H. Gutbrod et al., Nucl.Phys. **A397**(1982)177c.
52. G. Bertsch and J. Cugnon, unpublished, cited in ref. 53.
53. J. Cugnon, in "Heavy Ion Colisions", edited by P. Bonche et al., Plenum Press, New York (1986), p. 209.
54. L.D. Landau and E.M. Lifshitz, "Fluid Mechanics", Pergamon Press, Oxford (1959).
55. H. Stöcker, J. Maruhn and W. Greiner, Z.Phys. **A286**(1978)121.
56. G. Buchwald et al., Phys.Rev. **C24**(1981)135.
57. G. Buchwald et al., Phys.Rev. **C28**(1983)1119.
58. G. Buchwald et al., Phys.Rev.Lett. **52**(1984)1594.
59. M.I. Sobel, P.J. Siemens, J.P. Bondorf and H.A. Bethe, Nucl.Phys. **A251** (1975)502.
60. A.A. Amsden, G.F. Bertsch, F.H. Harlow and J.R. Nix, Phys.Rev.Lett. **35**

(1975)905.
61. J.R. Nix and D. Strottman, Phys.Rev. **C23**(1981)2548.
62. Y. Kitazoe and M. Sano, Prog.Theor.Phys. **54**(1975)922.
63. Y. Kitazoe and M. Sano, Prog.Theor.Phys. **54**(1975)1575.
64. G.F. Bertsch, in "Progress in Particle and Nuclear Physics", vol. 4, ed. by D. Wilkinson, Pergamon, Oxford (1980), p. 483.
65. J. Cugnon and D. L'Hôte, Nucl.Phys. **A447**(1985)27c.
66. N. Balazs, B. Schürmann, K. Dietrich and L.P. Csernai, Nucl.Phys.**A424** (1984)605.
67. R.E. Meyer, "Introduction to Mathematical Fluid Dynamics", J. Wiley, New-York (1971).
68. H.Å. Gustafsson et al., Phys.Rev.Lett. **52**(1984)1590.
69. P. Danielewicz, Phys.Lett. **146B**(1984)168.
70. A. Bonasera, L.P. Csernai and B. Schürmann, Nucl.Phys. **A476**(1988)159.
71. P. Danielewicz and G. Odyniec, Phys.Lett. **157B**(1985)146.
72. I. Tanihata et al., Phys.Lett. **97B**(1980)363.
73. J. Cugnon and J. Vandermeulen, "Winter College on Fundamental Nuclear Physics", third volume, ed. by K. Dietrich et al., World Scientific, Singapore (1985), p. 1373.
74. Z. Fraenkel, Nucl.Phys. **A428**(1984)373c.
75. K.K. Gudima, V.D. Toneev, G. Röpke and H. Schulz, Phys.Rev.**C32** (1985)1605.
76. M. Gyulassy, K. Fraenkel and E.A. Remler, Nucl.Phys. **A402**(1983)596.
77. E.A. Remler, Ann.Phys. (N.Y.) **136**(1981)293.
78. E.A. Remler, Phys.Rev. **C25**(1982)2974.
79. H. Schulz, G. Röpke, K.K. Gudima and V.D. Toneev, Phys.Lett.**124B** (1983)458 ; Phys.Rev. **C34**(1986)1294.
80. K.K. Gudima and V.D. Toneev, Nucl.Phys. **A400**(1983)173c.
81. G.J. Matthews, B.G. Glagola, R.A. Moyle and V.E. Viola, Phys.Rev.**C25** (1982)2181.
82. S. Das Gupta, B.K. Jennings and J.I. Kapusta, Phys.Rev. **C26**(1982)274.
83. C. Gale and S. Das Gupta, Phys.Lett. **162B**(1985)35.
84. L.P. Csernai and J.I. Kapusta, Phys.Rep. **131**(1986)223.
85. J. Cugnon and R. Lombard, Nucl.Phys. **A422**(1984)635 ; Phys.Lett. **134B** (1984)392.
86. H.W. Barz and H. Iwe, Nucl.Phys. **A453**(1986)728.
87. T.J. Humanic, Phys.Rev. **C34**(1986)191.
88. A.D. Chacon et al., Phys.Rev.Lett. **60**(1988)780.
89. J. Cugnon and S.E. Koonin, Nucl.Phys. **A355**(1981)477.
90. S. Nagamiya et al., Phys.Lett. **81B**(1979)147.
91. M. Cahay, J. Cugnon and J. Vandermeulen, Nucl.Phys. **A411**(1983)524.
92. C. Gale, Phys.Rev. **C36**(1987)2152.
93. J. Aichelin et al., to appear in Phys.Rev.Lett.
94. J.D. Stevenson, Phys.Rev.Lett. **45**(1980)1773.
95. G.N. Agakishiev et al., Sov.J.Nucl.Phys. **37**(1983)559.
96. K.K. Gudima et al., Nucl.Phys. **A467**(1987)759.
97. Y. Kitazoe et al., Phys.Rev. **C29**(1984)828.
98. Y. Kitazoe et al., Phys.Rev.Lett. **58**(1987)1508.
99. J. Cugnon and D. L'Hôte, Nucl.Phys. **A397**(1983)519.
100. J.R. Nix, D. Strottman, Y. Yariv and Z. Fraenkel, Phys.Rev.**C25** (1982)2491.
101. H. Stöcker et al., Phys.Rev.Lett. **47**(1981)1807.
102. R. Brockmann, Phys.Rev.Lett. **53**(1984)2012.
103. M. Anikina et al., Phys.Rev. **C33**(1986)895.
104. G.N. Agakishiev et al., Sov.J.Nucl.Phys. **40**(1984)767.
105. R. Stock, Phys.Rep. **135**(1986)259.
106. A. Sandoval et al., Phys.Rev.Lett. **45**(1980)874.
107. J.W. Harris et al., Phys.Lett. **153B**(1985)377.
108. J.W. Harris et al., Proc. of the 7th High Energy Heavy Ion Study, GSI, Darmstadt, Oct. 8-12 (1984).
109. E.L. Medeiros, S.J.B. Duarte and T. Kodama, Phys.Lett. **203B**(1988)205.
110. D. L'Hôte et al., Phys.Lett. **198B**(1987)139.
111. T.L. Ainsworth et al., Nucl.Phys. **A464**(1987)740.
112. B. ter Haar and R. Malfliet, Phys.Rev.Lett. **59**(1987)1652 ; Phys.Rev. **C36** (1987)1611.
113. G.R. Gulkanyan et al., Sov.J.Nucl.Phys. **40**(1984)479.
114. V.S. Barashenkov, F.G. Zheregi and Zh.Zh. Musul'manbekov, Sov.J.Nucl.Phys. **39**(1984)715.
115. V. Boldea et al., Sov.J.Nucl.Phys. **44**(1986)94.
116. R.E. Renfordt et al., Phys.Rev.Lett. **53**(1984)763.
117. R. Stock, Nucl.Phys. **A434**(1985)537c.
118. H. Stöcker and W. Greiner, Phys.Rep. **137**(1986)277.
119. G. Buchwald et al., Phys.Rev. **C28**(1983)2349.
120. M. Gyulassy, K.A. Fraenkel and H. Stöcker, Phys.Lett. **110B**(1982)185.
121. J. Cugnon, J. Knoll, C. Riedel and Y. Yariv, Phys.Lett. **109B**(1982)167.
122. E. Braun and Z. Fraenkel, Phys.Rev. **C33**(1986)120.
123. Y. Kitazoe et al., Phys.Rev.Lett. **53**(1984)2000.
124. H.G. Ritter et al., Nucl.Phys. **A447**(1985)3c.
125. J.J. Molitoris et al., Phys.Rev. **C33**(1986)867.
126. J.J. Molitoris and H. Stöcker, Phys.Rev. **C32**(1985)346.
127. B.P. Bannik et al., Z.Phys. **A329**(1988)341.
128. D. Beavis et al., Phys.Rev. **C33**(1986)1113.